Plant Cell Rep (2013) 32:1855–1867
DOI 10.1007/s00299-013-1498-y

ORIGINAL PAPER

# A knockdown mutation of *YELLOW-GREEN LEAF2* blocks chlorophyll biosynthesis in rice

**Hong Chen · Zhijun Cheng · Xiaoding Ma · Han Wu · Yanling Liu · Kunneng Zhou · Yilin Chen · Weiwei Ma · Jingcui Bi · Xin Zhang · Xiuping Guo · Jiulin Wang · Cailin Lei · Fuqing Wu · Qibing Lin · Yuqiang Liu · Linglong Liu · Ling Jiang**

Received: 1 July 2013 / Revised: 9 August 2013 / Accepted: 26 August 2013 / Published online: 17 September 2013


**Abstract**

***Key message*** **An insert mutation of *YELLOW-GREEN LEAF2*, encoding *Heme Oxygenase 1*, results in significant reduction of its transcript levels, and therefore impairs chlorophyll biosynthesis in rice.**

*Abstract* Heme oxygenase (HO) in higher plants catalyzes the degradation of heme to synthesize phytochrome precursor and its roles conferring the photoperiodic control of flowering in rice have been revealed. However, its involvement in regulating rice chlorophyll (Chl) synthesis is not fully explored. In this study, we isolated a rice mutant named *yellow-green leaf 2* (*ygl2*) from a $^{60}$Co-irradiated population. Normal grown *ygl2* seedlings showed yellow-green leaves with reduced contents of Chl and tetrapyrrole intermediates whereas an increase of Chl *a*/*b* ratio. Ultrastructural analyses demonstrated grana were poorly stacked in *ygl2* mutant, resulting in underdevelopment of chloroplasts. The *ygl2* locus was mapped to chromosome 6 and isolated via map-based cloning. Sequence analysis indicated that it encodes the rice HO1 and its identity was verified by transgenic complementation test and RNA interference. A 7-Kb insertion was found in the first exon of *YGL2/HO1*, resulting in significant reduction of *YGL2* expressions in the *ygl2* mutant. *YGL2* was constitutively expressed in a variety of rice tissues with the highest levels in leaves and regulated by temperature. In addition, we found expression levels of some genes associated with Chl biosynthesis and photosynthesis were concurrently altered in *ygl2* mutant. These results provide direct evidence that *YGL2* has a vital function in rice Chl biosynthesis.

**Keywords** Heme oxygenase-1 · Map-based cloning · Yellow-green leaves · Chloroplast · Chl biosynthesis · Rice

**Abbreviations**

| | |
|---|---|
| ALA | 5-Aminolevulinate |
| Proto IX | Protoporphyrin IX |
| Mg-Proto IX | Mg-Protoporphyrin IX |
| Pchlide | Protochlorophyllide |
| Chlide | Chlorophyllide |
| GFP | Green fluorescent protein |
| RNAi | RNA interference |
| RT-PCR | Reverse transcription polymerase chain reaction |
| qRT-PCR | Quantitative RT-PCR |
| ChlH Mg | Chelatase H subunit |
| ChlI | Mg-chelatase I subunit |
| ChlD | Mg-chelatase D subunit |
| PORA | NADPH:Pchlide oxidoreductase |
| CAO1 | Chlide A oxygenase1 |

Communicated by Z.-Y. Wang.

H. Chen, Z. Cheng and X. Ma contributed equally to this work.

**Electronic supplementary material** The online version of this article (doi:10.1007/s00299-013-1498-y) contains supplementary material, which is available to authorized users.

H. Chen · H. Wu · Y. Liu · K. Zhou · Y. Chen · Y. Liu · L. Liu · L. Jiang (✉)
National Key Laboratory for Crop Genetics and Germplasm Enhancement, Jiangsu Plant Gene Engineering Research Center, Nanjing Agricultural University, Nanjing 210095, China
e-mail: jiangling@njau.edu.cn

Z. Cheng · X. Ma · W. Ma · J. Bi · X. Zhang · X. Guo · J. Wang · C. Lei · F. Wu · Q. Lin
National Key Facility for Crop Gene Resources and Genetic Improvement, Institute of Crop Science, Chinese Academy of Agriculture Sciences, Beijing 100081, China

| | |
|---|---|
| Cab1 | Chlorophyll *a-b* binding protein 1 |
| Cab2 | Chlorophyll *a-b* binding protein 2 |
| PsaA | PSI P700 apoprotein A |
| PsbA | Photosystem II protein A |

## Introduction

Chlorophyll (Chl) is a green pigment found in plants and cyanobacteria, which absorbs sunlight and uses its energy to synthesize carbohydrates from $CO_2$ and water. Chl molecules are specifically around photosystems that are embedded in the thylakoid membranes of chloroplasts (Fromme et al. 2003). Heme is a vital component required for both photosynthesis and respiration (Terry and Kendrick 1996). HO1 converts heme to BV-IXα with the release of iron ($Fe^{2+}$) and carbon monoxide (CO) (Terry et al. 1993, 1995; Weller et al. 1996). Disruption of HO1 may indirectly affect chlorophyll biosynthesis, because both heme and chlorophyll branches share same substrates from 5-aminolevulinic acid to protoporphyrin IX (Weller et al. 1996). Chl and heme are two major tetrapyrroles of photosynthetic organisms in nature, and their metabolism has been extensively studied in various organisms such as cyanobacteria and *Arabidopsis thaliana* (von Wettstein et al. 1995; Grimm 1998). Analysis of the complete genome of *Arabidopsis* reveals that there are at least 27 genes encoding 15 enzymes involved in Chl biosynthesis (Nagata et al. 2005).

Rice (*Oryza sativa*) is a staple food crop for more than half of the world's population. Chl biosynthesis in rice plays a vital role to rice production. Chl-deficient mutants generally affect leaf colors, and are ideal genetic materials to investigate molecular mechanisms that regulate Chl biosynthesis and chloroplast development. More than ninety rice mutants were identified associated with leaf colors in a rice science database, for example, albino, chlorina, stripe (*st*), virescent (*v*) and zebra according to their phenotypes (http://www.shigen.nig.ac.jp/rice/oryzabaseV4/). Some of the genes underlying the mutations have been cloned. The *V1* mutant of rice develops chlorotic leaves under low-temperature condition and the *V1* gene encodes a chloroplast-localized protein NUS1, which promotes the establishment of the plastid genetic system during early chloroplast development in rice (Kusumi et al. 1997, 2011). The magnesium chelatase is a key enzyme catalyzing the chelation of $Mg^{2+}$ into proto IX to produce Mg-Proto IX, and it comprises three subunits (ChlH, ChlD and ChlI) (Jung et al. 2003; Davison et al. 2005). Mutations of the *Chlorina-1* and *Chlorina-9* genes encoding ChlD and ChlI subunits, respectively, lead to deficiency in Chl content and cause the incomplete development of chloroplasts (Zhang et al. 2006). The *Yellow-Green Leaf1* (*YGL1*) gene catalyzes esterification of chlorophyllide to complete the last step of Chl biosynthesis, and a missense mutation of which results in yellow-green leaves in young plants with decreased Chl synthesis and delayed chloroplast development (Wu et al. 2007). The *Young Seedling Albino* (*YSA*) encodes a protein with pentatricopeptide repeat and its mutation causes albino leaves before three-leaf stage in rice (Su et al. 2012). The *Young Leaf Chlorosis1* (*YLC1*) gene encodes a protein of unknown function belonging to the DUF3353 superfamily, disruption of which leads to a chlorosis phenotype at the seedling stage (Zhou et al. 2013). These above-mentioned genes provided useful information in uncovering Chl synthesis in rice.

In this study, we isolated a pigment-deficient mutant, which was induced by $^{60}Co$ γ-rays. The mutant exhibited a yellow-green leaf phenotype which was similar to *yellow-green leaf1* (*ygl1*) (Wu et al. 2007), and therefore was named *ygl2*. The *ygl2* mutant showed a reduction in Chl content and an obvious increase in the Chl *a*/*b* ratio. By map-based cloning, *ygl2* locus was isolated, and it encodes a plastid heme oxygenase (HO1). Genetic complementary experiments indicated *YGL2* could completely restore *ygl2* mutant phenotype. Our results provided the direct evidences that *YGL2* could play an important role to Chl biosynthesis in rice.

## Materials and methods

### Plant materials and growth conditions

The rice *ygl2* mutant was isolated from Gang 46B (*indica* type) by $^{60}Co$ radiation mutagenesis. All plants were grown in the experimental farms of the Institute of Crop Science in Beijing (China) during the natural growing season. For temperature treatments, the seedlings were grown in a growth chamber with 12/12 h (light/dark) at a constant air temperature of 23 °C (C23) or 30 °C (C30).

### Measurement of Chl and carotenoid (Car) contents

Chl and Car content were determined as the study described previously (Su et al. 2012). Equal weight of the second top leaf tissues was cut and suspended in 95 % ethanol for 48 h under dark conditions, and then centrifuged at 3,000*g* for 30 min to remove residual plant debris. The supernatants of these samples were analyzed with a SpectraMax Plus$^{384}$ spectrophotometer (Molecular Devices LLC, Sunnyvale, CA), and the concentrations of Chls and Cars were measured at 665, 649, and 470 nm and determined using the method of Lichtenthaler (1987).

### Transmission electron microscopy

To investigate the status of chloroplast development, leaf samples grown in growth chambers were harvested from 2-week-old days seedlings after germination. Leaf sections were fixed in a solution of 2 % glutaraldehyde and further fixed in 1 % $OsO_4$ overnight at 4 °C. Thereafter, they were stained with uranyl acetate before dehydrating through an ethanol series, and then embedded in Spurr's medium prior to thin sectioning. Samples were stained again and viewed with a Hitachi H-7650 transmission electron microscope.

### Map-based cloning of *ygl2*

For map-based cloning of *ygl2* gene, a mapping population was constructed by a cross between the *ygl2* mutant (*indica*) and Nipponbare (*japonica*). Individual plants showing yellow leaf phenotype in the $F_2$ progeny were selected for a genetic linkage analysis. Molecular markers distributed throughout the rice genome (McCouch et al. 2002a, b) were chosen for preliminary mapping. New InDel (insertion and deletion) markers for fine mapping were developed based on the DNA sequences of *indica* and *japonica* whole genomes (Yu et al. 2002; International Rice Genome Sequencing Project 2005), and primer sequences were listed in Supplemental Table 1.

### Complementation test and RNA interference

For functional complementation of the rice *ygl2* mutant, a full-length cDNA fragment encoding *YGL2* was amplified by RT-PCR with primers HO1-CF/HO1-CR, and then inserted into empty binary vector *pCUbi1390* through the Clontech In-Fusion® PCR cloning system (TaKaRa). The resulting *pUBI-YGL2* plasmid, which contained the *YGL2* coding sequence driven by the *ubiquitin* promoter and a *hygromycin* resistant marker, was transformed into *Agrobacterium tumefaciens* strain EHA105 by electroporation. Because *YGL2* mutant was originated from an *indica* variety, and its *calli* were validated to produce difficultly, a near isogenic line with *ygl2* allele in a *japonica* genetic background was obtained from *ygl2*/Nipponbare $F_3$ population using marker assistant selection. This line was further used as transforming receptor.

For RNAi experiments, the RNAi vector *pCUbi1390-*$\Delta FAD_2$ (Stoutjesdijk et al. 2002; Zhou et al. 2013) was fused with a 328 bp specific coding region of *YGL2*, which was amplified with primer pairs RNAi-SF/RNAi-SR and RNAi-AF/RNAi-AR (Supplemental Table 1). The resulting construct (*pUbi-RNAi-YGL2*) was transformed into *Agrobacterium tumefaciens* as described above. The empty vector *pCUbi1390* was used as a control. Kitaake, an easily regeneratable *japonica* variety, was chosen as transforming receptor. The protocol of *Agrobacterium tumefaciens*-mediated transformation in rice followed Hiei's previous study (Hiei et al. 1994).

### RT-PCR, qRT-PCR and histochemical assays

Total RNA was extracted from tissues of the wild type and *ygl2* mutant, respectively, using an RNA Prep Pure Plant kit (Tiangen Co. Beijing, China), and treated with DNase I following the manufacturer's instruction. The total cDNA was reverse transcribed using a SuperScript II kit (TaKaRa). The qRT-PCR analysis was performed using the ABI7500 Fast Real-Time PCR System with SYBR Premix Ex Taq kit (TaKaRa), and rice *ubiquitin* gene was chosen as endogenous control. Reactions containing SYBR premix were carried out in final volumes of 25 μl containing 0.2 μmol of the appropriate primers (Supplemental Table 1) and 1× SYBR green PCR master mix (PE Applied Biosystems). The $2^{-\Delta\Delta CT}$ method was used to calculate relative levels of gene expression (Schmittgen and Livak 2008). The primers for the *YGL2*, Chl biosynthesis and photosynthesis associated genes were given in Supplemental Table 1.

Histochemical β-glucuronidase (GUS) staining was performed according to methods described previously (Dai et al. 1996). Freshly collected samples from transgenic plants expressing the promoter-GUS fusion were put in the staining solution under vacuum-infiltrated for 30 min, and followed by incubation in darkness at 37 °C overnight. After staining, the samples were completely rinsed with 70 % ethanol and then photographed. Staining solution contained 50 mM sodium phosphate, 1 mM 5-bromo-4-chloro- 3-indolyl-b-D-glucuronide, 10 mM EDTA, 1 mM potassium ferrocyanide and 0.1 % [v/v] Triton X-100, pH 7.0.

### Subcellular localization

The full-length *YGL2* open reading frame (ORF) was amplified with primer pair GFP-F/GFP-R (see Supplemental Table 1) and ligated into binary vector *AHLG* under the control of the rice *ACTIN* promoter (Delaroche et al. 2010). Then the recombinant plasmid was introduced into Kitaake by *Agrobacterium tumefaciens*-mediated transformation. To exam the subcellular localization precisely, we isolated leaf protoplasts from those positive transgenic plants. Fluorescence of GFP was observed by a confocal laser scanning microscope (Leica TCS SP5).

### Determination of Chl precursors

Determination of ALA content was based on Richard's (1975) methods. The precursors of Chl synthesis pathway, including Proto IX, Mg-Proto IX, Pchlide, and Chlide, were assayed as described by Santiago-Ong et al. (2001)

and Masuda et al. (2003). Leaves (0.2 g fresh weight) of wild type and *ygl2* mutant were cut and homogenized in 5 mL 9:1 acetone:0.1 m$NH_4OH$, and centrifuged at 3,000*g* for 10 min. The supernatants were combined and washed three times successively with an equal volume of hexane prior to spectrophotometric analysis. Chl precursors in the acetone phase were quantified with a Hitachi F-4600 fluorescence spectrophotometer using Ex400:Em632 for Proto IX, Ex440:Em633 for Pchlide, Ex440:Em672 for Chlide, and Ex420:Em595 for Mg-Proto.

### Statistical analysis of the results

The data for comparison included at least three samples. *T* test was carried out using Microsoft Excel 2007 at significance level of 0.001, 0.01 or 0.05.

## Results

### The *ygl2* mutant shows reduced Chl content and less number of thylakoid lamellar in chloroplast

The *ygl2* mutant exhibited a yellow-green leaf phenotype when leaves emerged after germination. At three-leaf stage, the yellowish phenotype was the most obvious (Fig. 1a). Thereafter, from tiller initiating to heading stage, yellowish leaves gradually turned green and approached almost as normal as wild type did (Fig. 1b, c). In addition, the *ygl2* mutant showed a significant earlier flowering phenotype (near 20 days, $p < 0.001$) than that of wild type. Plant height is significantly lower than wild type throughout whole developmental stages (Supplemental Table 2) (*t* test, $p < 0.05$).

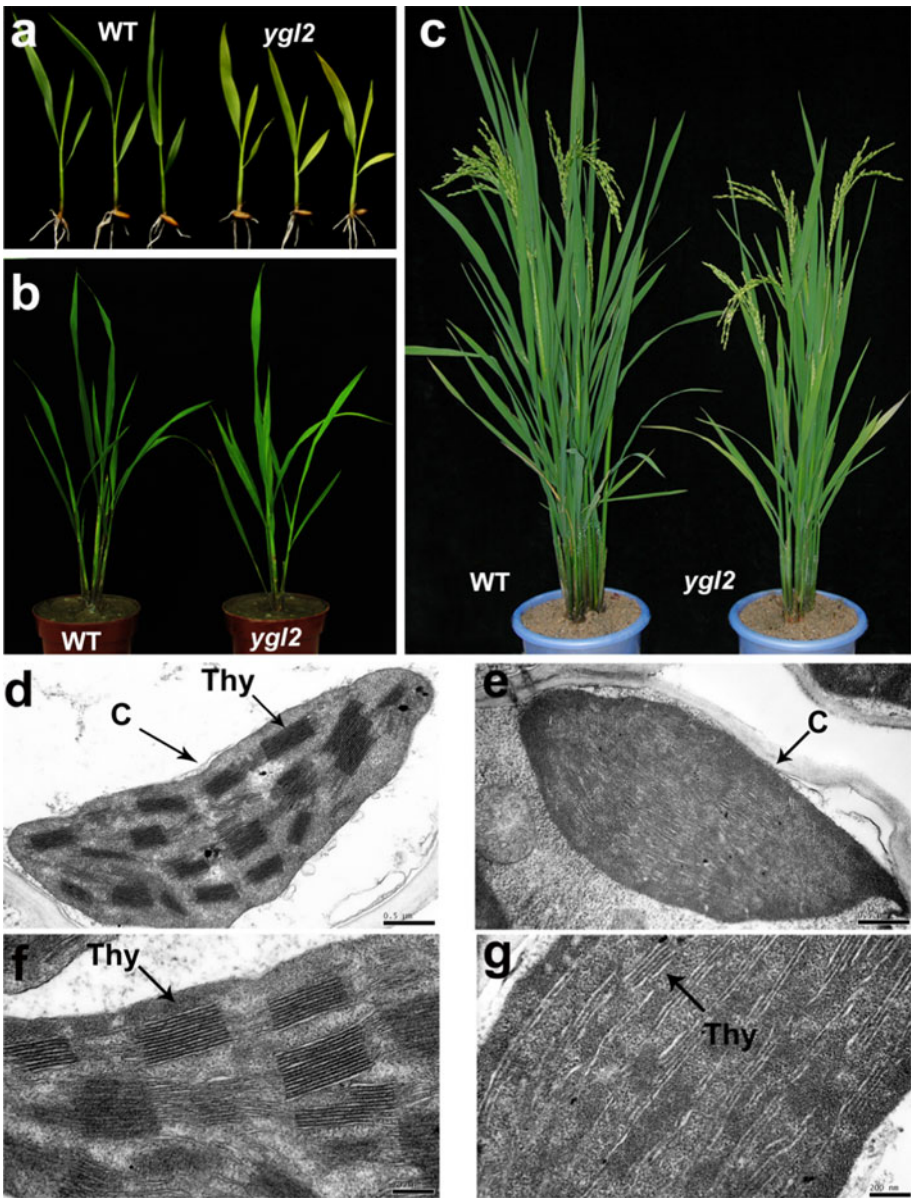


**Fig. 1** Phenotypic characterization of wild type (WT) and the rice *ygl2* mutant. **a** Leaf color of two-week-old WT and *ygl2* seedlings. **b** Leaf color of 6-week-old WT and *ygl2* seedlings. **c** Plants of WT and *ygl2* at the flowering stage. **d**, **e** Overview of chloroplast of wild type (**d**) and *ygl2* mutant (**e**) from 2-week-old plants. **f**, **g** Ultrastructures of chloroplasts in the mesophyll cells of WT (**d**) and *ygl2* mutant (**e**) plants from 2-week-old plants. *C* chloroplast, *Thy* thylakoid lamellar. *Bars* 0.5 μm (**d**, **e**), 0.2 μm (**f**, **g**)

Pigments contents at different developmental stages were examined and the results were showed in Table 1. At three-leaf stage, the *ygl2* mutant had a reduction of 37.7 % for Chl and 50 % for Car levels as compared to the wild type. During tillering stage, the percentages of Chl and Car reduction were narrowed to 19.4 and 24.5 % of normal levels, respectively. Compared to wild type, *ygl2* mutant showed higher Chl *a*/*b* ratio at three-leaf stage (*t* test, $p < 0.05$). The reduction of Chl contents and increase of Chl *a*/*b* ratio corresponded perfectly to yellowish scores of leaf colors.

To determine if *ygl2* mutation affects chloroplast development and morphology, we compared the ultrastructures of chloroplasts between the *ygl2* mutant and wild type plants at three-leaf stage using transmission electron microscopy. The number of thylakoid lamellar in chloroplasts of the *ygl2* was significantly less than that of wild type (Supplemental Fig. 1), whereas the structure of the thylakoid lamellar seemed normal and similar to that of wild type (Fig. 1d–g).

## The *YGL2* gene encodes a heme oxygenase on chromosome 6

Map-based cloning was used to isolate *ygl2* mutant gene. Initially, 190 individuals from the *ygl2*× Nipponbare $F_2$ population were used for genetic analysis. The phenotypic separation ratio fitted with 3:1 (150 normal: 40 yellow-green, $\chi^2 = 1.37 < \chi^2_{0.05,1} = 3.84$), suggesting the *ygl2* mutant phenotype was controlled by a single recessive gene. To map *ygl2* locus, 30 $F_2$ *ygl2*-like individuals were utilized. The *ygl2* gene was mapped to an interval between two InDel markers In9 and In11 on the long arm of chromosome 6 (Fig. 2a). 502 segregants showed mutant phenotype and were used for fine mapping; more markers were developed by comparing the difference of genomic sequences between *indica* and *japonica* whole genome. The *ygl2* locus was finally narrowed to a region of 66.8-kb between two InDel markers, In 44 and In 39 (Fig. 2a). Within the targeting region, there were eight recognizable open reading frames that were identified by Rice Genome Research Program (http://rgp.dna.affrc.go.jp/). Among these candidate genes, the sixth *ORF* (*Os06g40080*) encodes a heme oxygenase (HO1). Because a mutation of the *HO1* homolog in pea could cause pale foliage (Weller et al. 1996), we speculated that *Os06g40080* was likely the candidate gene underlying the *ygl2* phenotype.

To define the mutation(s) in *ygl2*, we sequenced genomic sequence of *Os06g40080* in *ygl2,* and found a fragment of 7-kb insertion in the first exon of *Os06g40080* (Fig. 2b, c). Based on exon/intron splicing rules (Black 2003), the 7-kb insertion was almost removed as the first intron (Fig. 2b). By sequencing RT-PCR product, a 46-bp insertion and 19-bp nucleotide deletion from codon 344 to 363 were detected in the mature transcript of *ygl2* (Supplemental Fig. 2a), leading to fifteen amino acids insertion and six amino acids deletion in putative protein (Supplemental Fig. 2b).

To confirm the identity of *YGL2/Os06g40080*, we performed a genetic complementation by expressing *Os06g40080* of wild type in the selected *ygl2* recessive homozygote of $F_3$ plant line. In the transgenic plants, all the characters including color of leaves (Fig. 3a), levels of Chl (Fig. 3b), and ratio of Chl *a*/*b* (Fig. 3c) were restored to the levels of wild type. In addition, we also constructed an RNAi vector of *YGL2* and transformed it into *japonica* variety Kitaake. A total of 12 positive transgenic plants displayed the similar phenotype as that in *ygl2* mutant (Fig. 3a). The expression levels of *YGL2* in leaves were consistent with the corresponding phenotypes in overexpression and RNAi plants (Supplemental Fig. 3). Taken together, we concluded that the abnormal phenotype of *ygl2* mutant resulted from the mutation of *YGL2* gene.

## YGL2 protein belongs to a highly conserved protein family and localized in chloroplast

Searching the rice genome database revealed that *YGL2* is a single-copy gene, and its coding sequence contains 870 nucleotides encoding a protein with 289 amino acids. Based on cDNA sequence analysis, the YGL2 protein has a calculated molecular mass of 31.9 KD with a putative transit peptide at its N-terminus. Research in the national center for biotechnology information (NCBI) (http://www.

**Table 1** Pigments contents in leaves of wild type and *ygl2* mutant, in mg $g^{-1}$ fresh weight

| Growth stage | Genotype | Total Chl | Chl *a*/*b* ratio | Car |
|---|---|---|---|---|
| Three-leaf stage | Wild type | 2.44 ± 0.21 | 3.32 ± 0.05 | 0.36 ± 0.03 |
| | *ygl2* | 1.52 ± 0.11** | 5.63 ± 0.14** | 0.18 ± 0.01** |
| Tillering stage | Wild type | 3.46 ± 0.25 | 3.45 ± 0.04 | 0.49 ± 0.07 |
| | *ygl2* | 2.79 ± 0.14** | 4.39 ± 0.06** | 0.37 ± 0.01** |

Chlorophyll (Chl) and carotenoid (Car) were measured in 95 % ethanol from the second leaf of different growth stages. Values are the mean ± SD ($n = 5$) (** $p < 0.01$)

ncbi.nlm.nih.gov/) revealed that both the wild type and mutant proteins contain a heme binding pocket and a heme ligand (Fig. 4). The HO1 encoded by *YGL2* has 67.8–97.8 % predicted amino acid sequence identity with other orthologs in higher plants (Supplemental Fig. 4 and Supplemental Fig. 5), suggesting it is a family member of highly conserved proteins. The mutation site in *ygl2* was resided in a relatively conserved region of *YGL2* (Supplemental Fig. 4). In addition, according to modeling of swissmodel (http://swissmodel.expasy.org/workspace), secondary and 3D structure of mutant ygl2 protein were compared with wild type. The results showed that ygl2 increased one additional $\beta$ strand in amino acid (AA) 105–110 but missed three *a*-helix in AA 45–52, 60–72, and 101–104, leading to disappearance of one loop and enlargement of another loop in tertiary structure (Fig. 4b).

To determine the subcellular localization of the YGL2 protein, the construct *YGL2-GFP* driven by rice *Actin* promoter was applied to transform rice plants. Confocal microscopy analysis of YGL2-GFP localization showed that GFP fluorescence overlapped with Chl auto fluorescence in isolated leaf protoplasts (Fig. 5), suggesting YGL2 is localized in chloroplast. To test whether the mutation in *ygl2* affected the subcellular localization, we also performed a transient expression analysis of the ygl2-GFP fusion protein. Most of ygl2 mutant proteins were localized in chloroplast (Supplemental Fig. 6), indicating the *ygl2* mutation did not affect protein anchoring.

## *YGL2* is constitutively expressed in various tissues and the *ygl2* mutation down-regulates its mRNA expression level

The qRT-PCR analysis was performed to study the expression profile of *YGL2*. As shown in Fig. 6a, the expression of *YGL2* was abundantly in flag leaf and penultimate leaf but relatively lower in root, culm, leaf sheath and young panicle. Compared with wild type, the expression level of *YGL2* was significantly decreased in various organs in *ygl2* mutant ($p < 0.05$, Fig. 6a), suggesting that

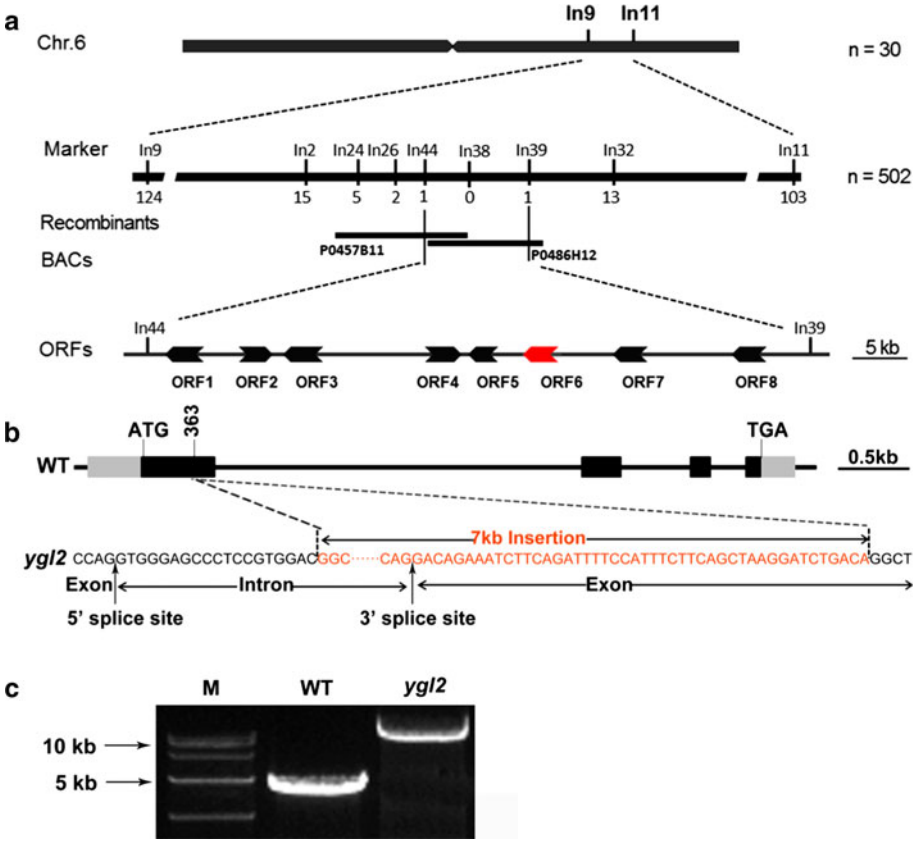


**Fig. 2** Map-based cloning of the *ygl2* gene. **a** Fine mapping of *ygl2* locus. The *ygl2* was first mapped to a region between the markers In 9 and In 11 on the long arm of rice chromosome (Chr) 6 with 30 recessive individuals. Then it was narrowed to a 66.8 kb region between the In 44 and In 39 using 502 recessive individuals from $F_2$ population. Eight open reading frames (ORFs) were predicted in the mapped region. **b** *YGL2* gene structure modeling. *Black boxes* indicate the coding sequence, *gray boxes* the 5′- and 3′-UTRs, and lines between boxes introns. ATG and TGA represent the start and stop codons, respectively. The *red letters* represent the 7-kb insertion which was almost removed as the first intron in the mature transcript of *ygl2*, and *black letters* denote wild type sequences. The *black arrows* represent splicing sites. **c** Identification of the genomic DNA fragment between wild type and *ygl2*. *M* molecular weight marker

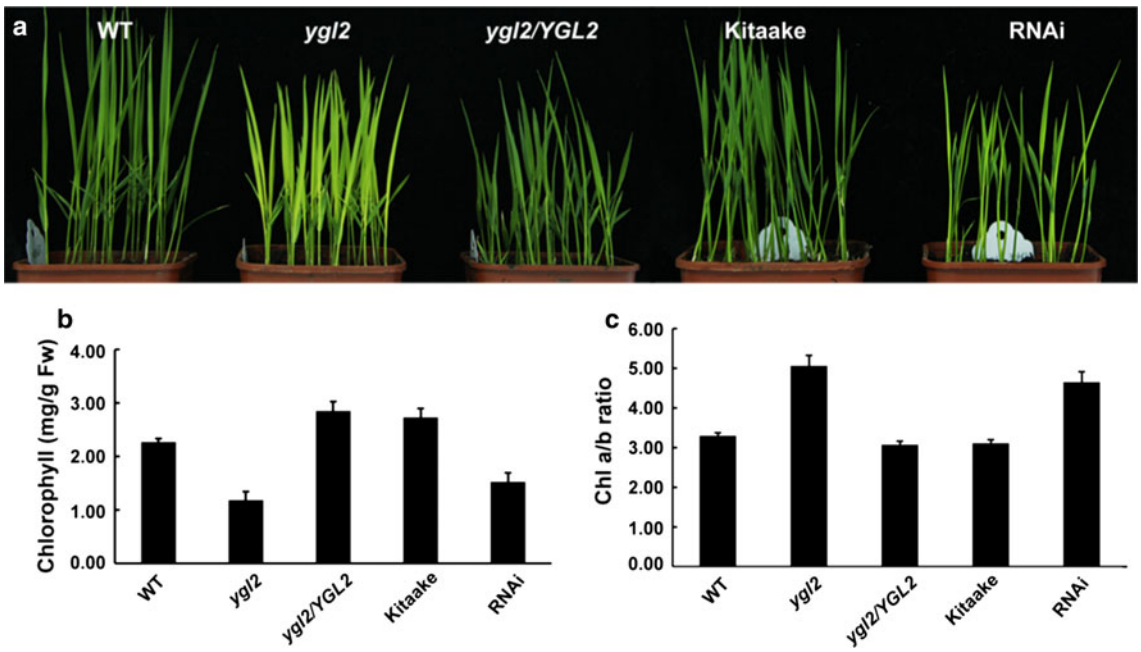


**Fig. 3** Functional complementation and RNAi knock-down analysis of *YGL2*. **a** Leaf color of a representative wild type (WT), *ygl2* mutant, a representative transgenic plant (*ygl2/YGL2*), control (Kitaake) and RNAi line, respectively. **b** Total chlorophyll (Chl) levels of the plants shown in (**a**). Chl was extracted from the second leaf of three-leaf-old plants. **c** Chl *a*/*b* ratio calculated from **b**. Values are the mean ± SD ($n = 3$)

the 7-kb insertion in the first exon obviously reduced the expression of *YGL2* in mutant. To verify qRT-PCR results, we further used transgenic plants carrying the *YGL2* promoter-GUS fusion construct to detect the *YGL2* endogenous expression level. GUS signals were detected in root, culm, leaf, leaf sheath and young panicle (Fig. 6b–e), and their relative strengths were consistent with expression pattern from qRT-PCR analysis.

A paralogue of *OsHO1* (named *OsHO2*) was also analyzed. The results showed that in wild type, the transcripts of both *OsHO1* and *OsHO2* at seedling stage were much higher than those at tillering stage. While in *ygl2*, the tendency was reversed (Fig. 6f, g).

## *YGL2* is temperature sensitive and affects expression of other genes associated with Chl biosynthesis and photosynthesis

To research whether the phenotype of *ygl2* was affected by temperature, we treated *ygl2* and wild type seedlings at two different temperatures. The yellowish color of *ygl2* became more obvious and the difference of Chl content between *ygl2* and wild type was even more significant at low temperature (23 °C) than high temperature (30 °C) (Fig. 7a, b). From 30 to 23 °C, the leaf color of wild type showed no obvious change, though their Chl levels had a reduction of 15.6 %. In contrast, significant color changes were observed in the *ygl2* leaves, and their Chl levels had a reduction of 45.6 % (Fig. 7c), indicating *ygl2* a temperature sensitive mutant. In wild type, *YGL2* expression levels at 23 °C were 6.6-fold higher than those at 30 °C treatment. While in mutant, *YGL2* exhibited only modest up-regulation (2.7-fold increase) at 23 °C, as compared with those at 30 °C (Fig. 7d).

The expression of ten genes associated with Chl biosynthesis (*CHLD*, *CHLI*, *CHLH*, *YGL1*, *PORA*, and *CAO1*) and photosynthesis (*Cab1*, *Cab2*, *PsaA* and *PsbA*) was analyzed to investigate their possible regulations by *YGL2*. At 30 °C, all tested genes in *ygl2* were significantly up-regulated as compared to wild type. Among them, *Cab1* showed the most obvious increase. Along with temperature decreased, most detecting genes in *ygl2* showed down-regulated trends except *CHLH* (Fig. 7e, f). The results indicated that *YGL2* gene played an important role in the regulation network of Chl biosynthesis and photosynthesis.

## Reduced expression of *YGL2* results in decreased intermediates of Chl biosynthesis

HO1 encoded by *YGL2* catalyzes the degradation of heme to form biliverdin IXα, a precursor of phytochrome (Cornejo et al. 1992; Weller et al. 1996). It was reported that heme accumulation could feedback inhibit Chl synthesis (Terry and Kendrick 1999). To detect whether the

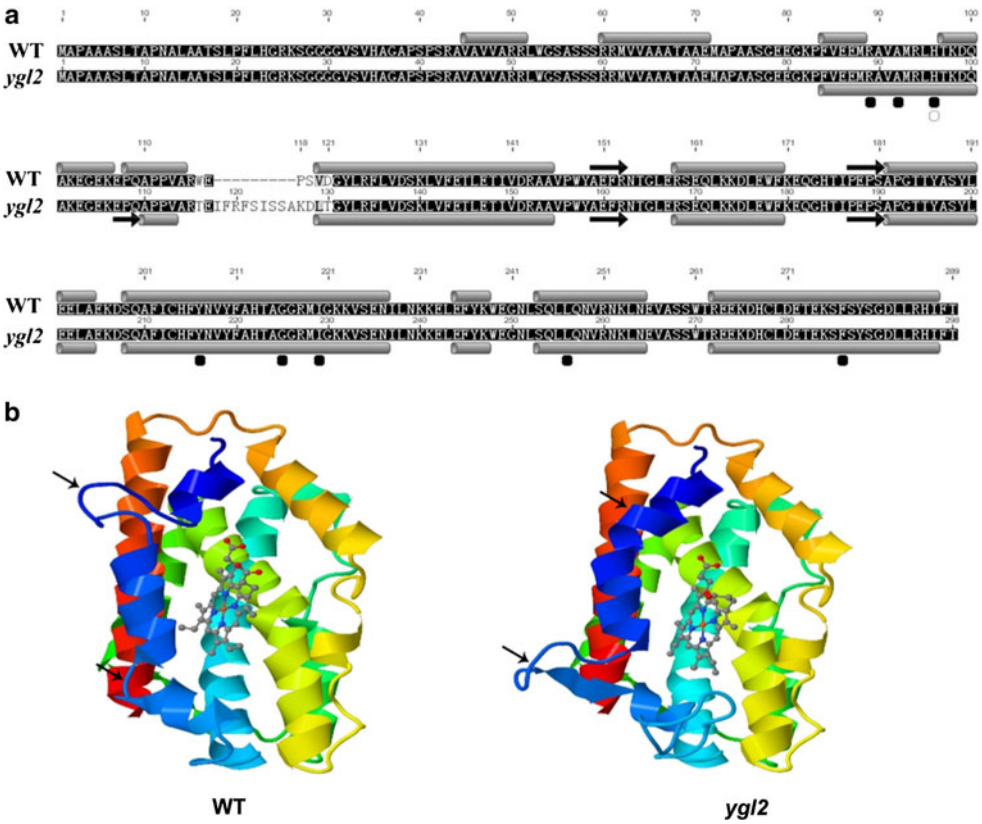


**Fig. 4** Structure comparison of the predicted protein between YLG2 and ygl2. **a** The alignment of complete amino acid sequence of the YGL2 and its mutant ygl2. The heme binding pocket and heme ligand sites are marked by solid and empty circles, respectively. Identical residues are demonstrated in shade. *Bars* indicate the positions of helices within the WT and ygl2 protein. *Arrows* indicate the positions of $\beta$ strands within the WT and ygl2 protein. **b** Docking structure of YGL2 and heme. The model was constructed according to the swissmodel (http://swissmodel.expasy.org/workspace). The ball-and-stick model structure indicates a heme molecular was embedded in both proteins of WT and *ygl2*. The difference of 3D-structure is showed by *arrows*

reduction of Chl resulted from the feedback inhibition of heme accumulation, we tested key intermediates in Chl biosynthesis by absorption spectroscopy. The results showed that *ygl2* had significantly decreased levels of protochlorophyllide (Pchlide) and Chlide as compared with wild type ($p < 0.05$) (Fig. 8). In contrast, no significant difference was found between mutant and wild type in other intermediates of Chl biosynthesis including ALA, proto IX and Mg- proto IX.

## Discussion

Heme is a vital component of the electron transport chains required for photosynthesis and degraded in the plastid through HO (Terry and Kendrick 1996). To date, genes encoding HOs have been isolated from a wide variety of organisms including animals, higher plants, red algae, cyanobacteria, and pathogenic bacteria (Ortiz de Montellano and Wilks 2001; Terry et al. 2002; Balestrasse et al. 2008). Structural analysis of HO revealed that it is a single compact domain consisting of mostly α-helices (Liu and Hu 2011). In higher plants, heme oxygenases are involved in the pathway leading to phytochrome chromophore metabolism, which was thought to be important in photoresponse, protection against oxidative stress and tissue injury, and lateral root formation (Terry et al. 1993, 2002; Ortiz de Montellano and Wilks 2001; Quail 2002a, b; Xie et al. 2012; Chen et al. 2013).

In this study, we described a rice mutant with yellow-green leaf color, *ygl2*. Map-based cloning is a powerful tool to isolate mutant gene(s) and has been widely used in various plants (Jander et al. 2002). Through fine mapping, an *ORF* encoding a HO was preliminary chosen from several candidates for further verification. Mutants with yellowish leaves caused by defects of *HO*s had been identified in other species. The *phytochrome chromophore-deficient 1* (*pcd1*) mutant of pea demonstrated pale yellow-green foliage and elongated internodes, and is caused by *HO1* deficiency (Weller et al. 1996; Linley et al. 2006). The *hy1* mutants in *Arabidopsis* showed partially etiolated morphology and three independent alleles of *hy1* all carried

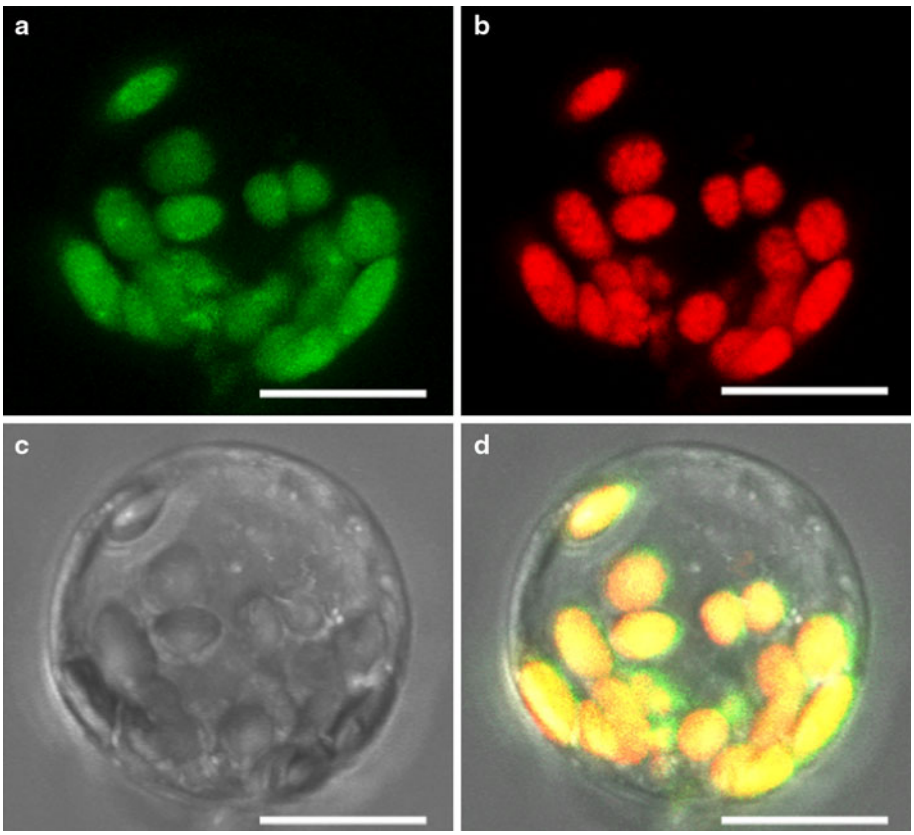


**Fig. 5** Subcellular localization of YGL2. **a** Fluorescence of YGL2 mostly located in the chloroplast of rice protoplasts. **b** Chlorophyll auto fluorescence. **c** Bright field. **d** Merged image of **a**, **b** and **c**. *Bar* indicates 10 μm

nucleotide substitutions/deletions within transcript region of *AtHO1* (Muramoto et al. 1999; Davis et al. 1999). The *yellow-green-2* (*yg2*) mutants of tomato had reduced Chl and anthocyanin, which resulted in a pale-green or yellow looking plants (Koornneef et al. 1985). Through high pressure liquid chromatography-based assay, it proposed *HO* dysfunction was responsible for *yg2* mutant phenotype (Terry and Kendrick 1996, 1999). Together these studies provided a strong hint that *ygl2* is probably encoded by a *HO*, whose mutation (s) as other ones in higher plants affects Chl synthesis and leaf color.

Sequence analysis indicated a 7-kb fragment was inserted in *YGL2* from *ygl2*. Previous studies showed that *YGL2/OsHO1* is a phytochrome synthesis factor, *SE5*, to control flowering in rice (Izawa et al. 2000; Andres et al. 2009). However, in *se5* the revertible yellow-green phenotype showing in *ygl2* was not focused on (Izawa et al. 2000; Andres et al. 2009). Besides the lesion of leaf color, *ygl2* also showed decreased plant height and early flowering (Supplemental Table 2), which is phenotypically similar to *se5* as a photochrome-deficient mutant (Andres et al. 2009). These results suggest *YGL2* has a pleiotropic effect to plant development. Here we addressed the Chl biosynthesis and chloroplast structure regulated by *YGL2*.

Chl contents (including Chl *a* and *b*) are required for the formation of photosynthetic reaction centers and light-harvesting complexes, whereas an appropriate ratio of Chl *a* and *b* is critical in the regulation of photosynthetic antenna size (Oster et al. 2000). In the *ygl2*, a decrease of Chl contents and an increase of Chl *a*/*b* ratio were observed, indicating both photosystems and light-harvesting antenna complexes might be impaired, just like another rice Chl-deficient mutant (*ygl1*, Wu et al. 2007). Granal stacks of the *ygl2* mutant appeared less dense (Fig. 1e, g) and decreased granal membranes as compared to wild type (Fig. 1d, f). It has long been established that mutations leading to defects in chlorophyll biosynthesis have a profound effect on the structure of plastids (Von Wettstein et al. 1995). The reduction of Chl synthesis and abnormal Chl *a*/*b* may disrupt the thylakoid ultrastructure in the mutant, which result in the reduction of filling of light-harvesting complexes in the thylakoid membrane. A Chl-deficient rice mutant has been reported to impair plastid development (Wu et al. 2007).

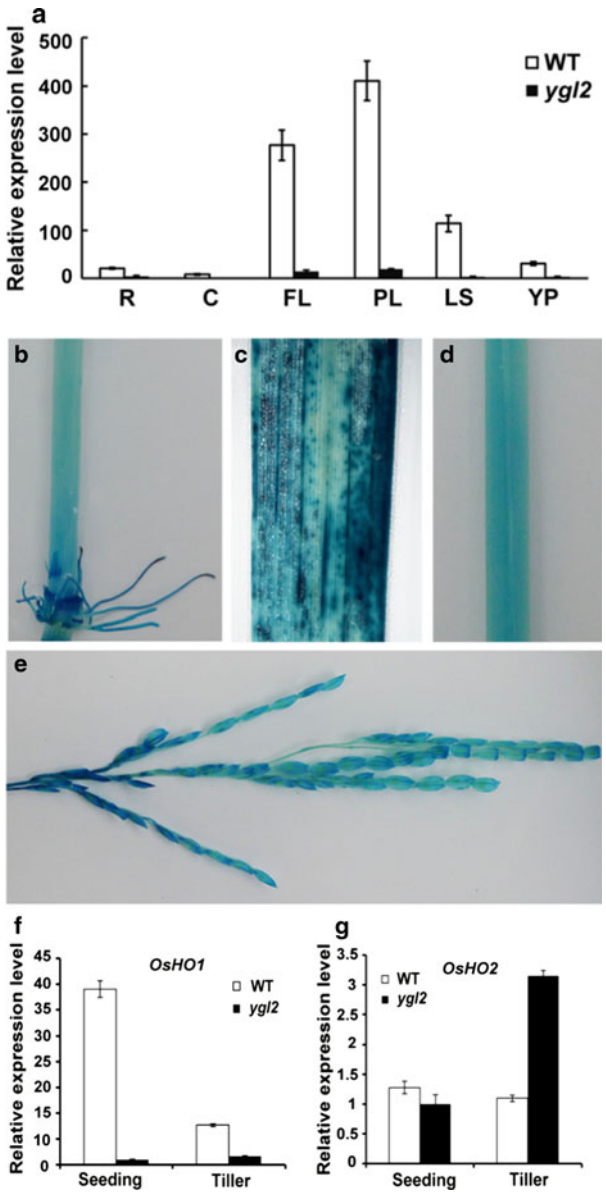


**Fig. 6** Expression analysis of *YGL2* by qRT-PCR. **a** Expression patterns of *YGL2* in root (R), culms (C), flag leaves (FL), the penultimate leaves (PL), leaf sheaths (LS), young panicles (YP) of wild type and *ygl2* mutant. **b–e** *YGL2* expression patterns of various tissues as revealed by GUS assay of *pYGL2-GUS* transgenic plants before heading. **b** Culms and roots. **c** Flag leaves. **d** Leaf sheaths. **e** Young panicles. **f** Expression level of *OsHO1* in the leaves of 3-week-old seedlings and tillering stage of plants, respectively. **g** Expression level of *OsHO2* in the leaves of 3-week-old seedlings and tillering stage of plants, respectively. *Ubiquitin* gene was amplified as a control. Values are mean ± SD ($n = 3$)

Transient expression indicated YGL2 from wild type and the mutant was both located in chloroplasts, suggesting the transit peptide of YGL2 in *ygl2* mutant is functional and sufficient to transport proteins to plastids. The mutation was resided in a relatively conservative region of YGL2, which affected the higher structure of putative protein (Fig. 4), thus might impair enzyme activity. We tried to purify YGL2 proteins in vitro through *Escherichia coli* and compare their differences of enzyme activities between mutant and wild type, but were unsuccessful. Further studies maybe conducted to reveal the effect of the *ygl2* mutation on enzyme activity.

Our results showed that the *YGL2* was constitutively expressed in a variety of tissues, which is consistent with the trends observed for *Arabidopsis HY1* (Davis et al. 1999). The mutation of *YGL2* directly caused the reduction of its expressions in various tissues, suggesting *YGL2* is regulated at transcript levels. The phenotypic effect of *ygl2* is much more severe in seedlings, but *ygl2* mutant is relatively healthy and recovered to wild type in the later stages of plant development. The presence of *OsHO2*, which is supposed to be functionally similar to *YGL2* in enzymatic reaction(s) and abundantly expressed later than *YGL2*, is expected to have responsibility in plant later development.

Both Chl and heme are synthesized by photosynthetic organisms (Grimm 1998). The biosynthesis pathway for Chl is common to holophytochrome synthesis from 5-aminolevulinic acid to protoporphyrin IX (Terry et al. 1995). It has been reported in other Chl-deficient mutants, the expressions of Chl biosynthesis and photosynthesis related genes were lower than those in wild type (Wu et al. 2007; Chai et al. 2011; Zhou et al. 2013). In contrast, these genes were up-regulated in *ygl2* mutant at normal air temperature. A simple explanation is, despite the *ygl2* mutation on phytochrome synthesis pathway, Chl biosynthesis and photosynthesis pathway are relatively functional. Therefore, plants can remedially up-regulate some genes related with the synthesis of Chl and photosynthesis and struggle to survive. In addition, negative feedback effect of free heme on ALA synthesis has been proposed (Chereskin et al. 1982; Terry and Kendrick 1999) and ALA synthesis is rate limiting for Chl synthesis in tomato (Beale and Weinstein 1991). The inability of YGL2/OsHO1 caused by *ygl2* mutation should lead to, more or less, heme accumulation, which then blocks Chl synthesis by feedback inhibition.

Our results showed *ygl2* had significantly decreased levels of protochlorophyllide (Pchlide) and Chlide, but no effects to other intermediates of Chl biosynthesis, such as Mg-proto IX and proto IX. These results are a little bit difference to those in a tomato *HO* mutant (*yg2*), which showed reduced effects of *yg2* to synthesize not only Pchlide but also Mg-proto IX (Terry and Kendrick 1999). This suggests *YGL2* has a function slightly divergent from its counterpart in tomato.

In conclusion, the results presented here indicate that *YGL2* in rice encodes a heme oxygenase required for Chl

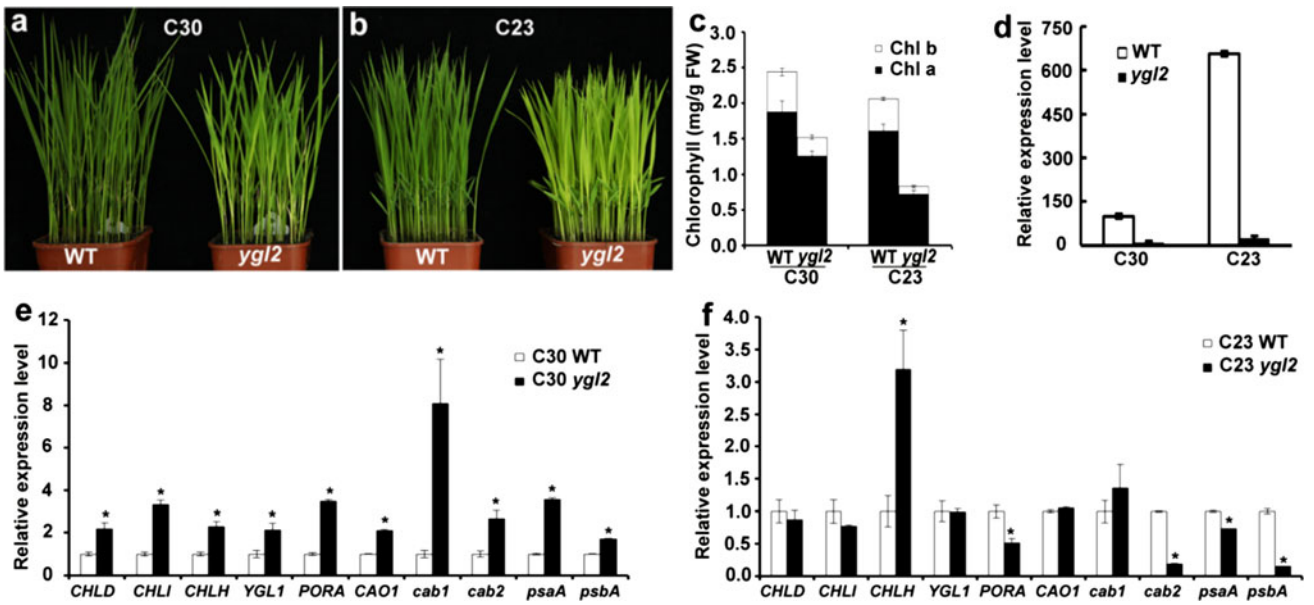


**Fig. 7** Quantitative PCR (qPCR) expression analysis of *YGL2* under temperature treatments and the genes associated with Chl biosynthesis and photosynthesis in WT and *ygl2* at 23 °C(C23) or 30 °C(C30), respectively. **a** Leaf phenotypes of wild type and *ygl2* mutant in 2-weeks-old seedlings grown at C30, 12 h light/12 h darkness. **b** Leaf phenotypes of wild type and *ygl2* mutant in 2-weeks-old seedlings grown at C23, 12 h light/12 h darkness. **c** Chlorophyll *a*/*b* contents at C30 and C23. **d** qPCR analysis of *YGL2* transcript levels in wild type and *ygl2* mutant at C30 and C23. Total RNA was isolated from leaves. **e** qPCR analysis of genes associated with Chl biosynthesis and photosynthesis in WT and *ygl2* at C30. **f** qPCR analysis of the genes associated with Chl biosynthesis and photosynthesis in WT and *ygl2* at C23. Total RNA was extracted from leaves of 2-week-old plants at C30 and 3-week-old at C23. *Ubiquitin* gene was amplified as a control. Values are the mean ± SD ($n = 3$) (*$p < 0.05$)

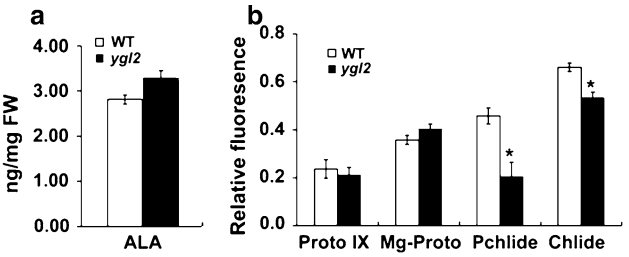


**Fig. 8** Analysis of chlorophyll (Chl) intermediates in wild type and *ygl1* mutant. Chl intermediates were measured in second leaf from 2-week-old wild type and *ygl2* mutant. **a** Levels of 5-aminolevulinate (ALA). *FW* fresh weight. **b** Contents of Proto IX, Mg-proto IX, Pchlide, and Chlide. Values are the mean ± SD ($n = 3$) (*$p < 0.05$)

biosynthesis. Molecular cloning of *YGL2* may provide a new prospect to analyze regulation of Chl biosynthesis pathway during rice developmental process.

**Acknowledgments** We thank Dr. Wenbiao Shen (Nanjing Agricultural University) for his help in Heme oxygenase activity. This research was supported by the grants from the 863 program of China (2011AA10A101, 2012AA101101). National Transform Science and Technology Program (2011ZX08001-004). Jiangsu Science and Technology Development Program (BK2010016, BE2012303). Jiangsu Province Self-innovation Program (CX(12)1003) and Qing Lan Project.

**Conflict of interest** The authors declare that they have no conflict of interest.

## References

Andres F, Galbraith DW, Talon M, Domingo C (2009) Analysis of *PHOTOPERIOD SENSITIVITY5* sheds light on the role of phytochromes in photoperiodic flowering in rice. Plant Physiol 151:681–690

Balestrasse KB, Yannarelli GG, Noriega GO, Batlle A, Tomaro ML (2008) Heme oxygenase and catalase gene expression in nodules and roots of soybean plants subjected to cadmium stress. Biometals 21:433–441

Beale SI, Weinstein JD (1991) Biochemistry and regulation of photosynthetic pigment formation in plants and algae. In: Jordan PM (ed) Biosynthesis of Tetrapyrroles. Elsevier, Amsterdam, pp 155–235

Black D (2003) Mechanisms of alternative pre-messenger RNA splicing. Ann Rev Biochem 72:291–336

Chai CL, Fang J, Liu Y, Tong HN, Gong YQ, Wang YQ, Liu M, Wang YP, Qian QA, Cheng ZK, Chu CC (2011) ZEBRA2, encoding a carotenoid isomerase, is involved in photoprotection in rice. Plant Mol Biol 75:211–222

Chen YH, Chao YY, Hsu YY, Kao CH (2013) Heme oxygenase is involved in $H_2O_2$-induced lateral root formation in apocynin-treated rice. Plant Cell Rep 32:219–226

Chereskin BM, Wong YS, Castelfranco PA (1982) In vitro synthesis of the chlorophyll isocyclic ring : transformation of Magnesium-Protoporphyrin IX and Magnesium-Protoporphyrin IX Monomethyl Ester into Magnesium-2,4-Divinyl Pheoporphyrin A(5). Plant Physiol 70:987–993

Cornejo J, Beale SI, Terry MJ, Lagarias JC (1992) Phytochrome assembly. The structure and biological activity of 2(R),3(E)-phytochromobilin derived from phycobiliproteins. J Biol Chem 267:14790–14798

Dai Z, Gao J, An K, Lee JM, Edwards GE, An G (1996) Promoter elements controlling developmental and environmental regulation of a tobacco ribosomal protein gene L34. Plant Mol Biol 32:1055–1065

Davis SJ, Kurepa J, Vierstra RD (1999) The *Arabidopsis thaliana HY1* locus, required for phytochrome-chromophore biosynthesis, encodes a protein related to heme oxygenases. Proc Natl Acad Sci USA 96:6541–6546

Davison PA, Schubert HL, Reid JD, Iorg CD, Herou XA, Hill CP, Hunter CN (2005) Structural and biochemical characterization of Gun4 suggests a mechanism for its role in chlorophyll biosynthesis. Biochemistry 44:7603–7612

Delaroche D, Cantrelle FX, Subra F, Van Heijenoort C, Guittet E, Jiao CY, Blanchoin L, Chassaing G, Lavielle S, Auclair C, Sagan S (2010) Cell-penetrating peptides with intracellular actin-remodeling activity in malignant fibroblasts. J Biol Chem 285:7712–7721

Fromme P, Melkozernov A, Jordan P, Krauss N (2003) Structure and function of photosystem I: interaction with its soluble electron carriers and external antenna systems. FEBS Lett 555:40–44

Grimm B (1998) Novel insights into the control of tetrapyrrole metabolism of higher plants. Curr Opin Plant Biol 1:245–250

Hiei Y, Ohta S, Komari T, Kumashiro T (1994) Efficient transformation of rice (*Oryza sativa* L.) mediated by Agrobacteriumand sequence analysis of the boundaries of the T-DNA. Plant J 6:271–282

International Rice Genome Sequencing Project (2005) The map-based sequence of the rice genome. Nature 436:793–800

Izawa T, Oikawa T, Tokutomi S, Okuno K, Shimamoto K (2000) Phytochromes confer the photoperiodic control of flowering in rice (a short-day plant). Plant J 22:391–399

Jander G, Norris SR, Rounsley SD, Bush DF, Levin IM, Last RL (2002) Arabidopsis map-based cloning in the post-genome era. Plant Physiol 129:440–450

Jung KH, Hur J, Ryu CH, Choi Y, Chung YY, Miyao A, Hirochika H, An G (2003) Characterization of a rice chlorophyll-deficient mutant using the T-DNA gene-trap system. Plant Cell Physiol 44:463–472

Koornneef M, Cone JW, Dekens RG, O'Herne-Robers EG, Spruit CJP, Kendrick RE (1985) Photomorphogenic responses of long hypocotyl mutants of tomato. J Plant Physiol 120:153–165

Kusumi K, Mizutani A, Nishimura M, Iba K (1997) A virescent gene *V1* determines the expression timing of plastid genes for transcription/translation apparatus during early leaf development in rice. Plant J 12:1241–1250

Kusumi K, Sakata C, Nakamura T, Kawasaki S, Yoshimura A, Iba K (2011) A plastid protein NUS1 is essential for build-up of the genetic system for early chloroplast development under cold stress conditions. Plant J 68:1039–1050

Lichtenthaler HK (1987) Chlorophylls and carotenoids:Pigments of photosynthetic biomembranes. Methods Enzymol 148:350–382

Linley PJ, Landsberger M, Kohchi T, Cooper JB, Terry MJ (2006) The molecular basis of heme oxygenase deficiency in the pcd1 mutant of pea. FEBS J 273:2594–2606

Liu R, Hu JJ (2011) HemeBIND: a novel method for heme binding residue prediction by combining structural and sequence information. BMC Bioinform 12:207

Masuda T, Fusada N, Oosawa N, Takamatsu K, Yamamoto YY, Ohto M, Nakamura K, Goto K, Shibata D, Shirano Y, Hayashi H, Kato T, Tabata S, Shimada H, Ohta H, Takamiya K (2003) Functional analysis of isoforms of NADPH: protochlorophyllide oxidoreductase (POR), PORB and PORC, in *Arabidopsis thaliana*. Plant Cell Physiol 44:963–974

McCouch SR, Teytelman L, Xu Y, Lobos KB, Clare K, Walton M, Fu B, Maghirang R, Li Z, Xing Y, Zhang Q, Kono I, Yano M, Fjellstrom R, DeClerck G, Schneider D, Cartinhour S, Ware D, Stein L (2002a) Development and mapping of 2240 new SSR markers for rice (Oryza sativa L.). DNA Res 9:199–207

McCouch SR, Teytelman L, Xu Y, Lobos KB, Clare K, Walton M, Fu B, Maghirang R, Li Z, Xing Y, Zhang Q, Kono I, Yano M, Fjellstrom R, DeClerck G, Schneider D, Cartinhour S, Ware D, Stein L (2002b) Development and mapping of 2240 new SSR markers for rice (*Oryza sativa* L.) (supplement). DNA Res 9:257–279

Muramoto T, Kohchi T, Yokota A, Hwang IH, Goodman HM (1999) The Arabidopsis photomorphogenic mutant *hy1* is deficient in phytochrome chromophore biosynthesis as a result of a mutation in a plastid heme oxygenase. Plant Cell 11:335–347

Nagata N, Tanaka R, Satoh S, Tanaka A (2005) Identification of a vinyl reductase gene for chlorophyll synthesis in Arabidopsis thaliana and implications for the evolution of Prochlorococcus species. Plant Cell 17:233–240

Ortiz de Montellano PR, Wilks A (2001) Heme oxygenase structure and mechanism. Adv Inorg Chem 51:359–407

Oster U, Tanaka R, Tanaka A, Rü diger W (2000) Cloning and functional expression of the gene encoding the key enzyme for chlorophyll b biosynthesis (CAO) from Arabidopsis thaliana. Plant J 21:305–310

Quail PH (2002a) Photosensory perception and signalling in plant cells: new paradigms? Curr Opin Cell Biol 14:180–188

Quail PH (2002b) Phytochrome photosensory signalling networks. Nat Rev Mol Cell Biol 3:85–93

Richard AT (1975) Biochemical spectroscopy, vol 1. Adam Hilger Ltd, London, pp 327–330

Santiago-Ong M, Green RM, Tingay S (2001) *shygrl1* is a mutant affected in multiple aspects of photomorphogenesis. Plant Physiol 126:587–600

Schmittgen TD, Livak KJ (2008) Analyzing real-time PCR data by the comparative C(T) method. Nat Protoc 3:1101–1108

Stoutjesdijk PA, Singh SP, Liu Q, Hurlstone CJ, Waterhouse PA, Green AG (2002) hpRNA-mediated targeting of the *Arabidopsis FAD2* gene gives highly efficient and stable silencing. Plant Physiol 129:1723–1731

Su N, Hu ML, Wu DX, Wu FQ, Fei GL, Lan Y, Chen XL, Shu XL, Zhang X, Guo XP, Cheng ZJ, Lei CL, Qi CK, Jiang L, Wang H, Wan JM (2012) Disruption of a rice pentatricopeptide repeat protein causes a seedling-specific albino phenotype and its utilization to enhance seed purity in hybrid rice production. Plant Physiol 159:227–238

Terry MJ, Kendrick RE (1996) The *aurea* and *yellow-green-2* mutants of tomato are deficient in phytochrome chromophore synthesis. J Biol Chem 271:21681–21686

Terry MJ, Kendrick RE (1999) Feedback inhibition of chlorophyll synthesis in the phytochrome chromophore-deficient *aurea* and *yellow-green-2* mutants of tomato. Plant Physiol 119:143–152

Terry MJ, Wahleithner JA, Lagarias JC (1993) Biosynthesis of the plant photoreceptor phytochrome. Arch Biochem Biophys 306:1–15

Terry MJ, McDowell MT, Lagarias JC (1995) (3Z)- and (3E)-phytochromobilin are intermediates in the biosynthesis of the phytochrome chromophore. J Biol Chem 270:11111–11118

Terry MJ, Linley PJ, Kohchi T (2002) Making light of it: the role of plant heme oxygenases in phytochrome chromophore synthesis. Biochem Soc T 30:604–609

Von Wettstein D, Gough S, Kannangara CG (1995) Chlorophyll biosynthesis. Plant Cell 7:1039–1057

Weller JL, Terry MJ, Rameau C, Reid JB, Kendrick RE (1996) The Phytochrome-Deficient *pcd1* mutant of pea Is unable to convert heme to biliverdin IXα. Plant Cell 8:55–67

Wu Z, Zhang X, He B, Diao L, Sheng S, Wang J, Guo X, Su N, Wang L, Jiang L, Wang C, Zhai H, Wan J (2007) A chlorophyll-deficient rice mutant with impaired chlorophyllide esterification in chlorophyll biosynthesis. Plant Physiol 145:29–40

Xie Y, Xu D, Cui W, Shen W (2012) Mutation of *Arabidopsis HY1* causes UV-C hypersensitivity by impairing carotenoid and flavonoid biosynthesis and the down-regulation of antioxidant defence. J Exp Bot 63:3869–3883

Yu J, Hu S, Wang J, Wong GK, Li S et al (2002) A draft sequence of the rice genome (*Oryza sativa* L. ssp. *indica*). Science 296:79–92

Zhang H, Li JJ, Yoo J-H, Yoo S-C, Cho S-H, Koh H-J, Seo HS, Paek N-C (2006) Rice *Chlorina-1* and *Chlorina-9* encode ChlD and ChlI subunits of Mg-chelatase, a key enzyme for chlorophyll synthesis and chloroplast development. Plant Mol Biol 62:325–337

Zhou K, Ren Y, Lv J, Wang Y, Liu F, Zhou F, Zhao S, Chen S, Peng C, Zhang X, Guo X, Cheng Z, Wang J, Wu F, Jiang L, Wan J (2013) *Young Leaf Chlorosis 1*, a chloroplast-localized gene required for chlorophyll and lutein accumulation during early leaf development in rice. Planta 237:279–292